Photodynamic effect on melanoma cells investigated by atomic force microscopy

K. Tomankova[1], H. Kolarova[1], M. Vujtek[2] and R. Bajgar[1]

[1] *Department of Medical Biophysics, Faculty of Medicine, Palacky University in Olomouc, Hněvotínská 3, 775 15 Olomouc, Czech Republic*
[2] *Department of Experimental Physics, Faculty of Nature Science, Palacky University in Olomouc, tř. Svobody 26, 771 46 Olomouc, Czech Republic*

Abstract. Atomic force microscopy (AFM) is a modern experimental method for imaging of conducting or non-conducting samples. New trends in the application of scanning probe microscopy (SPM) give us the ability to scan live cells directly in their ingenuous surroundings or in air. Our apparatus was replenished with an inverse optical microscope, so we could observe the position of the scanning tip in every individual cell. The aim of the presented study is to picture the cell surface in air. A dry scanner in non-contact or tapping mode was used in the biological application of AFM. In our work the cell line G361 was used as a biological sample. We imaged the cell line before and after induction of a photodynamic effect (PDE) by irradiation of $ZnTPPS_4$-loaded cells with a light dose of 15 J/cm^2. Individual cells before PDE induction had a smooth surface without protrusion on the entire surface. Cells after PDE induction did not have a smooth surface but their surface was rough with protrusion and in some places cleaved.

Key words: Atomic force microscopy — Photodynamic effect — Melanoma cell — Sensitizer

Introduction

New trends in the application of scanning probe microscopy (SPM) give us the ability to scan live cells directly in their ingenuous surroundings or in special conditions like in air, vacuum, liquid or at low temperature (Morris and Kirby 1999; Langer et al. 2000). Atomic force microscopy is a versatile tool in the field of biological science (Fotiadis et al. 2002). Cell membranes and many biomolecules, including proteins and nucleic acids (Fujita et al. 2002; Yu et al. 2004), have been extensively imaged (Kienberger et al. 2003). Using AFM scanning of melanocytes and study of their properties is possible, too (Kemkemer et al. 2003). The utility of AFM strongly varies depending on the cell type, its membrane structure (Mendez-Vilas et al. 2004) and adhesion properties (Kim et al. 2003). The minimal forces between tip and surface of the sample avoid damage of the biological preparation (Dufrêne et al. 2001). Interactions between the cantilever tip and the cell surface are so complex that there is no simple way to control tip-cell interactions and to eliminate the disruptive effect of the scanning cantilever (You et al. 2000). In our experiment was used a dry scanner and cells were scanned in the non-contact or the tapping mode (Lehenkari et al. 2000). Non-contact AFM (NC-AFM) mode was developed for improving imaging of soft samples by AFM. Difficulties in the proper adjustment of the scanning parameters are often encountered when using tapping mode AFM (TM-AFM) for imaging thick and soft materials, and particularly living cells in aqueous buffer. To increase quality of our images, we scanned cells in NC-AFM mode (Vie et al. 2000). Recognition of the cells and control of their surrounding during imaging have already been accepted as essential conditions for cell biological application of AFM (Bolshakova et al. 2001).

Photodynamic therapy (PDT), originally developed and used mainly as a minimally invasive tumour therapy, has been known for over a hundred years (Kaestner 2003; Kessel 2004). In clinical PDT, dyes such as porphyrins (Mosa et al. 1997; Chen et al. 2005) or phthalocyanines are administered

Correspondence to: Katerina Tomankova, Department of Medical Biophysics, Faculty of Medicine, Palacky University in Olomouc, Hněvotínská 3, 775 15 Olomouc, Czech Republic
E-mail: tomanko@tunw.upol.cz

to a patient along with irradiation. PDT is predominantly used in anticancer treatment approaches that depend on the retention of photosensitizers in tumour cells and their activation within the tumour through irradiation with light of the appropriate wavelength (Dougherty 1993).

The aim of the present study is represent tumor cell surface in air by AFM. We focused to obtain topography pictures and pictures involving elastic properties of cell surface. We examined the cell line G361 before and after induction of photodynamic effect (PDE). Differences in altitude over surface of cells gave us information about cell damage and about different component parts of the cell wall (Kim et al. 2004).

Materials and Methods

Materials

Our experiments were performed on the G361 cell line (human melanoma cells) as a biological substrate using the following chemicals: Dulbecco´s modified eagle medium (DMEM – 10% fetal bovine serum, 1% penicillin-streptomycin, 1% glutamine), the photosensitizer $ZnTPPS_4$, ethanol, deionized water. Imaging was done using the AFM Explorer with a cover head (Veeco, USA) and an inverse fluorescent optical microscope Olympus IX70. Further we used sterile plastic microscope slides Thermanox® as substrates for samples and Petri dishes for cultivation of the cell line.

PDT

One million cells were placed on a plastic slide and put to the Petri dishes. Cells were incubated in culture medium DMEM at 37°C and 5% CO_2 with 20 μmol/l of the photosensitizer $ZnTPPS_4$ for 24 h. The first Petri dishes were used as a negative control (cells with culture medium only). The second part of the dishes represented cells in the presence of 20 μmol/l $ZnTPPS_4$ and irradiated with a dose of 15 J/cm^2. For irradiation we used light emitting diodes with the emission wavelength maximum at 417 nm. After irradiation, cells were cultured for 12 h at the same conditions as described above.

AFM

We imaged the cell line before and after photodynamic treatment, using a dry scanner at an image size of 100 × 100 μm. For details of the cell surface we used a scan-size of 2 × 2 μm (Doktycz et al. 2003). For the experiments we disposed the AFM Explorer microscope with a cover head. Furthermore, we exerted a non-contact tip from antimony doped silicon 1650-00, 125 μm long, 30 μm wide, 10–15 μm high of the tip and a spring constant of 42 N/m at a resonance frequency of 320 kHz (Veeco, USA). The radius of curvature of the sharpened probes was 20 nm (non-contact tip). We used an AFM scanner with hardware correction for non-linearities of the piezoelectric elements. The AFM surface images were acquired in non-contact mode either as topographies that show height of contours or as phase images that highlight the fine structure or surface morphology (Santos and Castanho 2004). A 100 × 100 μm scan with a resolution of 300 pixels line took between 5 and 10 min based on the scan rate. Critical in our experiments was the identification of the optimum cantilever amplitude, set point to image the soft cell surface without damage. For the optimum imaging the set point was found at about 50%

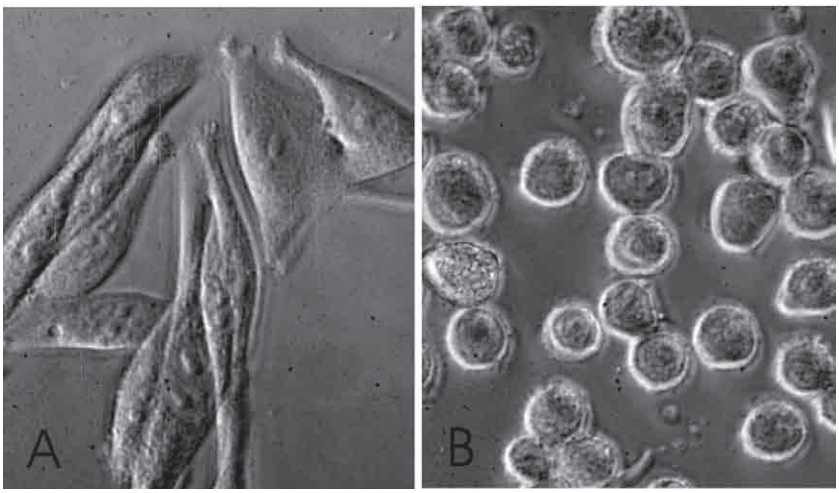

Figure 1. Human melanoma cells G361 observed in transmitted light-microscopy at 400× magnification. **A.** Control G361 cells without irradiation. **B.** Photodamaged G361 cells after PDT with $ZnTPPS_4$ (concentration 10 μmol/l, irradiation dose 15 J/cm^2).

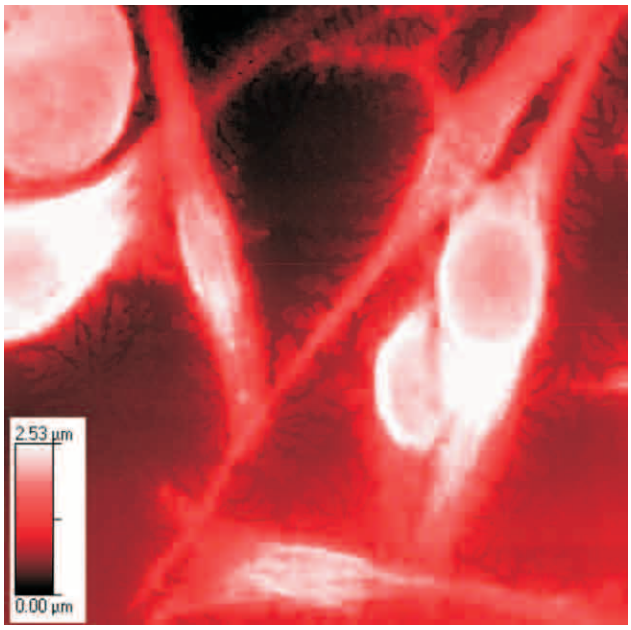

Figure 2. Cell line G361 before PDE induction. Undamaged adhered cells on substrate create clusters with cell extension (invadopodia) projecting toward other cells. The image was obtained in non-contact topography mode (size 100 × 100 μm, resolution 300 × 300 pixels, scan rate 80 μm/s). Height of cells is expressed in a colour scale from 0 (dark red) to 2.53 (white) μm.

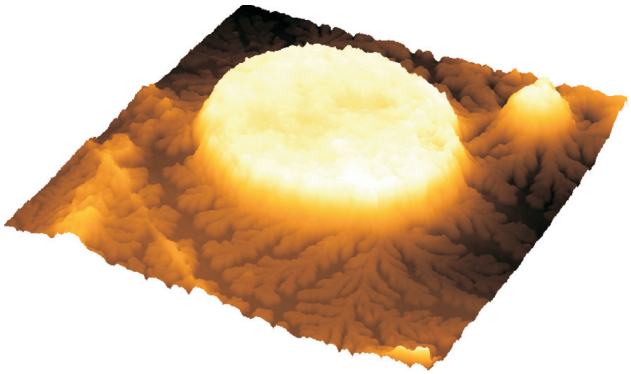

Figure 3. One non-irradiated cell of G361 cell line before PDE induction. The image was obtained in non-contact 3D topography mode (size 46 × 46 μm, resolution 300 × 300 pixels, scan rate 50 μm/s). Height of cell is expressed in colour scale from 0 (dark brown) to 2.13 (yellow) μm.

of vertical extent of scanner (Chasiotis et al. 2003). Proximity of the cantilever tip to the surface was identified by reduction of the oscillation amplitude valuable for imaging in air. AFM studies of soft materials are often conducted in liquid to increase cantilever damping and thus reduce

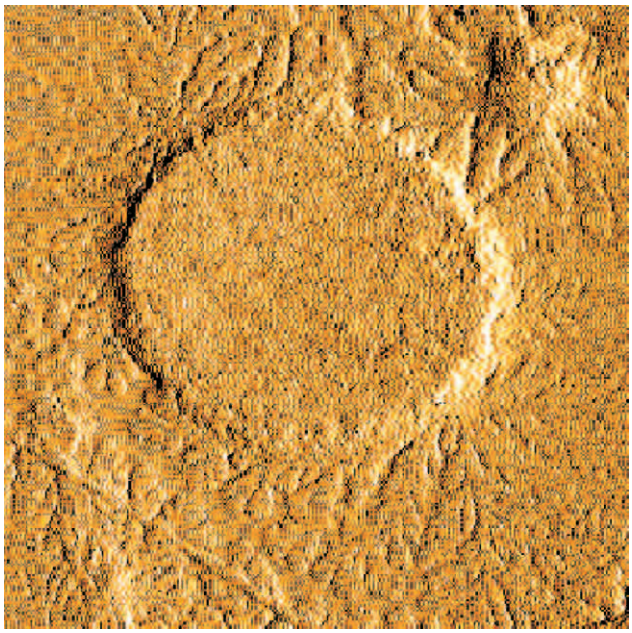

Figure 4. The image of cell line G361 before PDE in non-contact phase image mode (size 46 × 46 μm, resolution 300 × 300 pixels, scan rate 50 μm/s).

the local damage caused to cells. Images were processed by SPM Lab software.

Results

Using AFM we observed changes on G361 cells after induction of PDE induced by application of violet light at the dose of 15 J/cm^2 in the presence of 20 μmol/l $ZnTPPS_4$. Microscopical study (Fig. 1) shows morphological changes in cell cultures after photodynamic treatment. Fig. 1A presents undamaged control human melanoma cells G361 without irradiation; Fig. 1B shows photodamaged G361 cells after PDE with $ZnTPPS_4$ at concentration 20 μmol/l and dose of light irradiation 15 J/cm^2. The topography image of non-treated G361 cells is shown in Fig. 2. Undamaged cells adhered to substrate created clusters with cell extension (invadopodia) projecting toward other cells (Fillmore et al. 2003). The size of invadopodia was up to 70 μm long. Crystals of growth medium were found in the neighborhood of the cell. Cell samples were dried about half an hours and the presented figure shows typical shape of individual cell in the cluster. The G361 cells exposed to PDE were observed in both modes, the non-contact topography (Fig. 3) and the phase mode (Fig. 4). Randomly selected profiles were analyzed for each cell. The roughness of the cell surface was measured in horizontal, vertical and

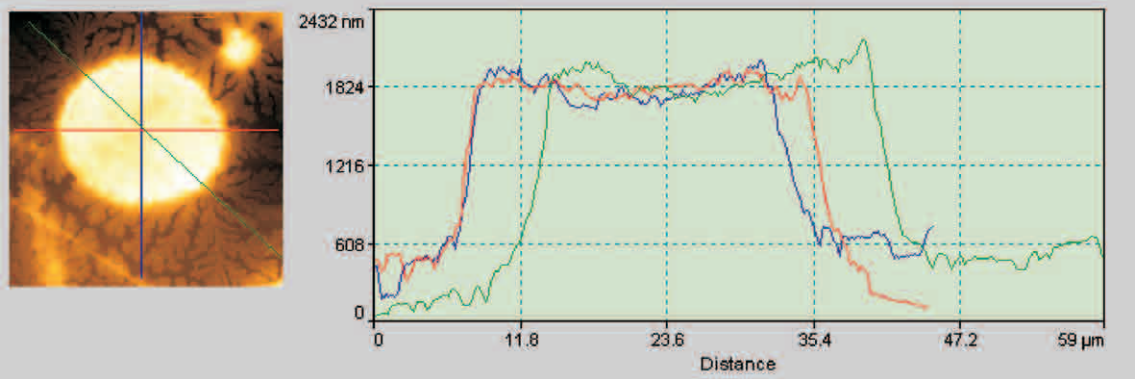

Figure 5. The surface profile of a G361 cell before PDE in horizontal (red curve), vertical (blue curve), and slant (green curve) direction.

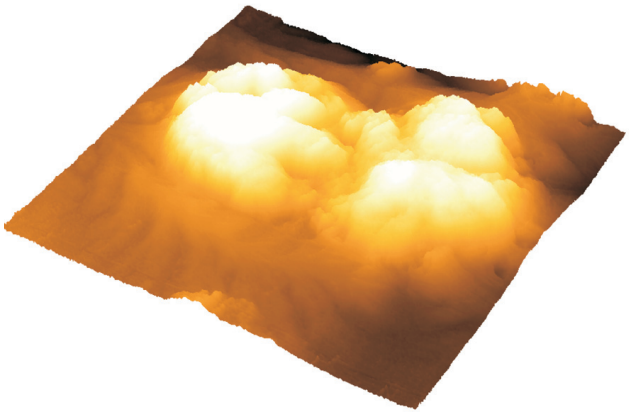

Figure 6. Two cells of the cell line G361 after induction of a PDE. The image was obtained in non-contact 3D topography mode (size 52 × 52 μm, resolution 300 × 300 pixels, scan rate 40 μm/s). Height of cells is in range from 0 (dark brown) to 1.83 (white) μm.

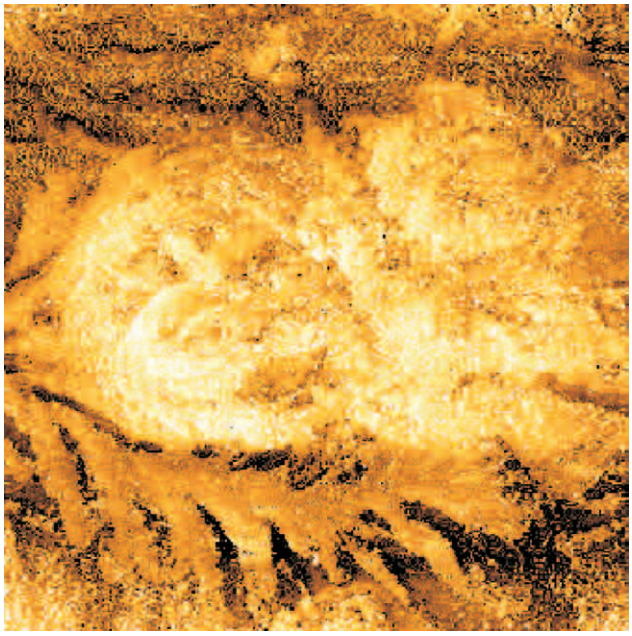

►

Figure 7. The representative G361 cell after induction of PDE. The typical characteristic of the cell is a rough surface. Image was obtained in non-contact phase image mode (size 52 × 52 μm, resolution 300 × 300 pixels, scan rate 40 μm/s).

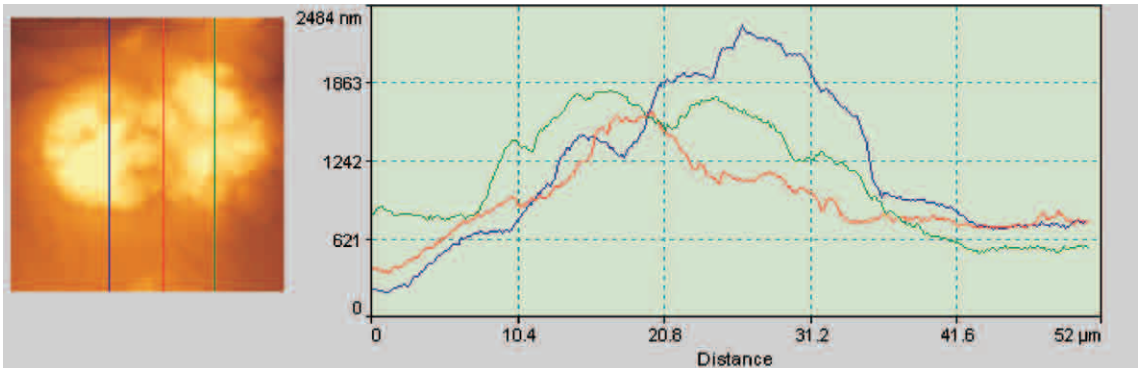

Figure 8. The surface profile of a G361 cell after PDE in vertical (red, blue and green curve) direction in various location.

slant line direction (Fig. 5). The profile of the cell surface in the three directions gives us information about shape and height of the cell. The size of the cell in Fig. 3 is 31 μm in length, 29 μm in width and 2.13 μm in height. These values show that the cell has an ellipsoidal shape. When we focus on each of these curves, we see that the surface of this cell is smooth. The deflection of the profile curves from a line is not more than 30 nm. The basis of the therapy is to create such conditions that lead to the destruction of cell membranes and so to cell death. The response to the photodynamic treatment is dependent on the photosensitizer used, irradiation conditions, oxidation status of the tissue, and cell-type involved. The G361 cells exposed to PDE were also imaged in both modes, the non-contact topography (Fig. 6) and the phase mode (Fig. 7). The size of the cell in Fig. 6 on the right side is 32 μm long and 24 μm wide, height of this cell is 1.83 μm. The length, width and height of the second cell in Fig. 6 is 30, 22 and 2.2 μm, respectively. The values show that the cells are geometrically in ellipsoidal shape again. Thus, the size of cells after irradiation is the same as before PDE. Changes can only be found in the roughness of their surfaces. The surface roughness of the PDE-exposed cell was measured in vertical direction only (Fig. 8). The measurement gives us information about the shape and height of the two G361 cells. When we focus on these lines, we see that the surface of these cells is not smooth, but on lines there are great differences in waveform – the deflection of the profile curves from a line is more than 200 nm. These results show that cells before photodynamic treatment have symmetrical shape and soft structure along the whole surface of cell in comparison with PDE-exposed cells. Their cover has a rough structure (see Fig. 8) and burst create after irradiation. The average distance between two prominences on the cell surface calculated for each profile of non-treated melanoma cells varied between 30–50 nm. After PDE induction, the distance increased to 200–400 nm (see Figs. 5 and 8). After data processing and their digitalizing, some of the artefacts were not removed in order to protect some morphological features of resulting cell images. High resolution images of cells were difficult to acquire, because the cells were soft and deformable. We can detect the efficiency of PDE and obtain important information about this treatment. The cells before induction of PDE are characterized by smooth surfaces without protrusion. In contrast, PDE-induced cells do not have smooth surfaces, but their membrane is rough with protrusion and cleaved.

Discussion

Scanning of the cells is limited by the construction of AFM (Moloney et al. 2002; Pyo et al. 2006). To overcome these limitations we added an inverse optical microscope to the AFM. The instrument provided us continuous observation of the tip during the scanning process of an individual cell (Berdyeva et al. 2005; Puech et al. 2006). We obtained two different types of cell pictures: topography and phase image, the letter giving more information about the topography. In general, the shape of the cells depends on the type and also on the state of cell; for example, dead cells are characterized by circular or elliptic shape in comparison with oblong shape of live cells with invadopodia. The high deformability of the soft cytoplasmatic membrane due to the interaction with the hard tip is the most important reason for the difficulty to obtain images of melanoma cells at all as well as the limited resolution of the presented images. Before the experiments, the DMEM was removed from the cells and optical microscopy was used to identify suitable cell candidates or clusters of cells for AFM examination in air (Nowakowski et al. 2001). AFM imaging was proceeded immediately after the removal of the nutrient media DMEM. Scanning was performed at high dry level (O´Reilly et al. 2001). The images presented here were obtained at the beginning of measurement sequence in each case. Tips were either new or cleaned by ethanol and deionized water and desiccated (Spatz et al. 1998). At the magnification of objects, most of the cell texturing was visible. Light areas in the presented images are places of cell elevation and dark areas correspond to cell depression. This fact is related to the hardness or softness of the sample. High areas seem to be harder while low areas could be the softer parts (Kim et al. 2003). Before photodynamic treatment, it was almost impossible to find some dead cell. The drying method used reflects morphology of the cells in stage closely before removing liquid. The live undamaged cells have elongate shape in comparison with photodynamically damaged cells. In this case, the term "live cell imaging" is really not exact and therefore we replaced or removed the adjective from the term, even if the cells look like live on the images. For comparison, cells were imaged before and after photodynamic treatment in order to observe changes on the cell surface after PDE induction. In contrast, it was almost impossible to find undamaged cells after induction of PDE. The porphyrine sensitizer $ZnTPPS_4$, often used in PDT, is mostly distributed in various membranous structures, where it induces oxidative damage after photoactivation (Baugh et al. 2001; Sun et al. 2003). In general, PDE on cells resulting in cell death depends on the kind of cell, chemical structure of sensitizer, its concentration, and irradiation conditions. The necrosis is accompanied with damage of the cell membrane integrity and metabolic homeostasis causing morphological changes like a swelling and burst of the membrane. The second type of the cell death, apoptosis, is characterized by a formation of apoptotic bodies, condensation of the nuclear chromatin and fragmentation of the DNA (Eum et al. 2007; Liao and Lieu 2005).

Acknowledgments. This work was supported by the Grant Project MSM 6198959216 and FRVS 20110291.

References

Baugh S. D. P., Yang Z., Leung D. K., Wilson D. M., Breslow R. (2001): Cyclodextrin dimers as cleavable carriers of photodynamic sensitizers. J. Am. Chem. Soc. **123**, 12488–12494

Berdyeva T., Woodworth C. D., Sokolov I. (2005): Visualization of cytoskeletal elements by the atomic force microscope. Ultramicroscopy **102**, 189–198

Bolshakova A. V., Kiselyova O. I., Filonov A. S., Yu O., Lyubchenko Y. L., Yaminsky I. V. (2001): Comparative studies of bacteria with an atomic force microscopy operating in different modes. Ultramicroscopy **86**, 121–128

Chasiotis I., Fillmore H. L., Gillies G. T. (2003): Atomic force microscopy observation of tumour cell invadopodia: novel cellular nanomorphologies on collagen substrates. Nanotechnology **14**, 557–561

Chen Z. H., Chen B., Lu Z. X., Pang D. W., Song Y. (2005): Assembling zwitterionic, water-soluble porphyrin and its biological studies. Wuhan University Journal of Natural Sciences **10**, 587–590

Doktycz M. J., Sullivan C. J., Hoyt P. R., Pelletier D. A., Wu S., Allison D. P. (2003): AFM imaging of bacteria in liquid media immobilized on gelatin coated mica surfaces. Ultramicroscopy **97**, 209–216

Dougherty T. J. (1993): Photodynamic therapy. Photochem. Photobiol. **58**, 895–900

Dufrêne Y. F., Boonaert J. P., van der Mei H. C., Busscher H. J., Rouxhet P. G. (2001): Probing molecular interactions and mechanical properties of microbial cell surfaces by atomic force microscopy. Ultramicroscopy **86**, 113–120

Eum H. A., Cha Y. N., Lee S. M. (2007): Necrosis and apoptosis: Sequence of liver damage following reperfusion after 60 min ischemia in rats. Biochem. Biophys. Res. Commun. (available online)

Fillmore H. L., Chasiotis I., Cho S. W., Gillies G. T. (2003): Atomic force microscopy observation of tumour cell invadopodia: novel cellular nanomorphologies on collagen substrates. Nanotechnology **14**, 73–76

Fotiadis D., Scheuring S., Müller S. A., Engel A., Müller D. J. (2002): Imaging and manipulation of biological structures with the AFM. Micron **33**, 38–397

Fujita M., Mizutani W., Gad M., Shigekawa H., Tokumoto H. (2002): Patterning DNA on μm scale on mica. Ultramicroscopy **91,** 281–285

Kaestner L. (2003): Evaluation of human erythrocytes as model cells in photodynamic therapy. Gen. Physiol. Biophys. **22**, 455–465

Kemkemer R., Csete M., Schrank S., Kaufmann D., Spatz J. (2003): The determination of the morphology of melanocytes by laser-generated periodic surface structures. Mater. Sci. Eng., C **23**, 437–440

Kessel D. (2004): Photodynamic therapy: from the beginning. Photodiag. Photodyn. Ther. **1**, 3–7

Kienberger F., Stroh C., Kada G., Moser R., Baumgartner R., Pastushenko V., Rankl C., Schmidt U., Müller H., Orlova E., Le Grimellec C., Drenckhahn D., Blaas D., Hinterdorfer P. (2003): Dynamic force microscopy imaging of native membranes. Ultramicroscopy **97**, 229–237

Kim H., Arakawa H., Osada T., Ikai A. (2003): Quantification of cell adhesion force with AFM: distribution of vitronectin receptors on a living MC3T3-E1 cell. Ultramicroscopy **97**, 359–363

Langer M. G., Koitschev A., Haase H., Rexhausen U., Hörber J. K. H., Ruppersberg J. P. (2000): Mechanical stimulation of individual stereocilia of living cochlear hair cells by atomic force microscopy. Ultramicroscopy **82**, 269–278

Lehenkari P. P., Charras G. T., Nykänen A., Horton M. A. (2000): Adapting atomic force microscopy for cell biology. Ultramicroscopy **82**, 289–295

Liao P. C., Lieu C. H. (2005): Cell cycle specific induction of apoptosis and necrosis by paclitaxel in the leukemic U937 cells. Life Sci. **76**, 1623–1639

Méndez-Vilas A., Corbacho I., González-Martín M. L., Nuevo M. J. (2004): Direct surface probing of cell wall-defective mutants of Saccharomyces cerevisiae by atomic force microscopy. Appl. Surf. Sci. **238**, 51–63

Moloney M., McDonnell L., O´Shea H. (2002): Immobilisation of Semliki forest virus for atomic force microscopy. Ultramicroscopy **91**, 275–279

Morris V. J., Kirby A. R., Guning A. P. (1999): Atomic Force Microscopy for Biologist. Imperial College Press, London

Mosa M., Zitko M., Pouckova P. (1997): Distribution and photodynamic effect of zinc phthalocyanine disulfonate in nude mice bearing mammary carcinoma. Neoplasma **44**, 178–183

Nowakowski R., Luckham P., Winlove P. (2001): Imaging erythrocytes under physiological conditions by atomic force microscopy. Biochim. Biophys. Acta **514**, 170–176

O´Reilly M. O., McDonnell L., Mullane J. O. (2001): Quantification of red blood cells using atomic force microscopy. Ultramicroscopy **86**, 107–112

Puech P. H., Poole K., Knebel D., Muller D. J. (2006): A new technical approach to quantify cell-cell adhesion forces by AFM. Ultramicroscopy **106**, 637–644

Pyo N., Tanaka S., McNamee C. E., Kanda Y., Fukumori Y., Ichikawa H., Higashitani K. (2006): Effect of the cell type and cell density on the binding of living cells to a silica particle: an atomic force microscope study. Colloids Surf., B: Biointerfaces **53**, 278–287

Santos N. C., Castanho M. (2004): An overview of the biophysical applications of atomic force microscopy. Biophys. Chem. **107**, 133–149

Spatz J. P., Sheiko S. S., Möller M. (1998): Shape and quality control of modified scanning force microscopy tips. Ultramicroscopy **75**, 1–4

Sun F., Hamagawa E., Tsutsui C., Sakaguchi N., Kakuta Y., Tokumaru S., Kojo S. (2003): Evaluation of oxidative stress during apoptosis and necrosis caused by D-galactosamine in rat liver. Biochem. Pharmacol. **65**, 101–107

Vie V., Giocondi M. C., Lesniewska E., Finot E., Goudonnet J. P., Le Grimellec C. (2000): Tapping-mode atomic force microscopy on intact cells: optimal adjustment of tapping conditions by using the deflection signal. Ultramicroscopy **82**, 279–288

You H. X., Lau J. M., Zhang S., Yu L. (2000): Atomic force microscopy imaging of living cells: a preliminary study of the disruptive effect of the cantilever tip on cell morphology. Ultramicroscopy **82**, 297–305

Yu M., Ivanisevic A. (2004): Encapsulated cells: an atomic force microscopy study. Biomaterials **25**, 3655–3662

Final version accepted: May 18, 2007